
Article:
Bournine, H., Wagg, D.J. and Neild, S.A. (2011) Vibration damping in bolted friction beam-columns. Journal of Sound & Vibration, 330 (8). 1665 - 1679. ISSN 0022-460X

https://doi.org/10.1016/j.jsv.2010.10.022

Vibration damping in bolted friction beam-columns

Hadjila Bournine , David J. Wagg, Simon A. Neild[1]

Department of Mechanical Engineering, University of Bristol, Bristol, U.K, BS8 1TR

Abstract

In this paper we consider dynamic friction within a bolted structure deliberately used to improve damping properties of the structure. The structure considered for this paper consists of two steel beam-columns bolted together allowing dynamic friction to occur at the interface. This paper includes an analysis of the behavior of the structure and the effect of friction on its dynamics. It also includes an analysis of the energy dissipation in the structure by means of friction and the optimization of the bolt tension in order to dissipate the maximum vibration energy by the structure. We define analytical expressions for the vibration behaviour before and after slip occurs as well as the point at which it starts. We also define the stress profile across the column cross-section. An experiment was designed to allow the measurement of the bolt tension, the slip within the structure and the bending velocity. The theoretical analysis gave very close agreement with the experimental results.

Key words: Friction, vibration damping, bolted columns.

1. INTRODUCTION

In this paper we consider the effect of friction on the dynamics of a vibrating beam-column. The results presented here are based on the idea of using bolted friction beam-columns to add damping during large amplitude motion. The set up consists of two steel beam-columns bolted together allowing dynamic friction to occur at the interface. This type of system has been shown to dissipate a large amount of vibration energy [1] when the bolt tensions are adjusted appropriately. The concept is similar to leaf springs which have been in practice for some considerable time [2]. Potential applications are structures with very low damping characteristics such as large steel structures (i.e. steel framed buildings). Consequently these structures are particularly sensitive to dynamic excitation from wind or seismic loading. In some cases relatively small loadings can induce considerable lateral vibration that can result in damage to the structure.

The usual approach to providing more damping in a structure is to add some form of structural dampers, which can be either passive or semi-active. For seismic applications a common way to apply more passive damping is in the form of base-isolation, which is achieved by using rubberised mounts to isolate the structure from its foundations. Other passive damping designs include special bracing mechanisms [3, 4] or devices fitted between columns and beams [5, 6, 7, 8] of the structure. Some of the semi-active damping

mechanisms based on friction are described in [9, 10, 11, 12]. An extended overview of a large part of the literature on friction damping systems is presented in [13, 14].

A similar system has been previously considered by Popp et al [1] where the optimum normal force required was defined based on the maximum dissipated energy. To work effectively, the bolted friction column must be designed with the appropriate bolt tensions to dissipate significant vibrational energy when dynamically excited. The friction damping effect only occurs when static friction at the interface of the beam-column is overcome, and can therefore be designed to happen only under large amplitude motion. For example for protecting the structure in extreme circumstances, such as an earthquake. At all other times the structure operates in its usual low damping regime. The potential advantages are that this method is simple, relatively cheap and reduces the need for active dampers or additional cross-bracing.

The theoretical analysis presented in this paper includes two physical approaches. The first one deals with the structural analysis of the beam-column. In Sec. 2.5 , we develop expressions for the vibration modes based on the dynamics of friction at the interface. The second approach (Sec. 2.3) is based on the optimum energy dissipation by the structure. We derive analytical expressions for the energy dissipated by friction and its effect on the vibration magnitude. To validate the analysis, we carry out a set of

experiments which we describe in section 3. The experimental results show a good agreement with the analytical predictions.

2. Analytical model

The bolted friction beam-column used in the following analysis involves two steel beams bolted together as shown in Fig. 1. It is assumed that the pressure applied by the bolts is approximated by a continuously distributed load along the beam-column.

2.1. Relative displacement

We consider the case of two steel columns, with rectangular cross-section, clamped back-to-back. When the clamped columns deflect, slip may occur along the interface between $beam_1$ and $beam_2$. This is a result of the difference in the beams radii of curvature due to their thickness as shown in Fig 2. Fig. 3(a) shows the relative displacement at the tip of the beam. u_i is the displacement of the centreline of $beam_i$ due to axial loading and w is the lateral deflection of the whole beam-column. Therefore, the relative displacement can be expressed as

$$u = u_2 - u_1 + w'T, \tag{1}$$

where w is the beam deflection, T is the distance between the centrelines of the beams, in the case of identical beams, it is also the thickness of each

one, and the dash " $'$ " represents partial differentiation with respect to x. This value will vary depending on the bolt tension applied as the higher the tension the less readily slip will occur. In the case of full slip, we assume compatibility in the beams deflection i.e. the central axes of the two beams are assumed to be at the same distance in the axial direction as shown in Fig. 3(b). Therefore, the only relative displacement along the column is due to the bending itself. In the case of full stick, there is no relative displacement at the interface as shown in Fig. 3(c). In the analysis only the cases of full stick or full slip will be considered. By differentiating Eq. 1 with respect to x to obtain the relative displacement distribution along the beam, we obtain

$$u' = \epsilon_2 - \epsilon_1 + w''T, \tag{2}$$

where ϵ is the strain due to the normal force,

$$\epsilon_i = P_i/E_iA_i, \tag{3}$$

P_i is the axial load of *beami* and A_i is the cross sectional area of *beami*.

2.2. Friction Model

The friction model assumed here is a Coulomb type model. The friction force at the interface $f(x)$ over a single period of vibration, is assumed to be a function of the relative displacement u between the two beams. As used by [1], the model relating $f(x)$ to u is shown in Fig. 4. The friction

hysteresis is approximated by a parallelogram with respect to the relative displacement, this is a reasonable approximation if the column is undergoing harmonic vibration. In all cases, the friction force is assumed to be linearly related to the relative displacement, therefore can be expressed as

$$f(x) = b + ku, \tag{4}$$

where b and k are constants that take different values depending on each stage of the hysteresis and u is the relative displacement between the two beams. In this paper two distinctive cases are considered, the first one is the case of full slip has $b = sign(\dot{x})\mu q(x)$, where μ is the friction coefficient and $q(x)$ is the normal load at the interface surfaces. The second case is the full slip phase.

2.3. Energy Balance Model

The energy considered in this case is the bending energy and the work done by friction. We assume that the viscous damping is negligible in comparison to the friction damping. All the assumptions made before are also assumed for this analysis.

We assume that the deflection of the beam can be described using the following equation

$$w = W\left(1 - \cos(\frac{\pi}{2l}x)\right), \tag{5}$$

where W is the time dependent deflection magnitude at the free end of the of the beam-column.

For our beam-column, the bending stiffness for a single beam is EI. Therefore the potential energy due to bending for the whole beam-column, is defined as

$$\begin{aligned} V_b &= 2\int_0^l \frac{1}{2} EI(w'')^2 dx \\ &= \frac{EI\pi^2}{32l}(W^2). \end{aligned} \tag{6}$$

Next, we define the energy dissipated by friction. For any structure, the work done by friction is defined as the product of the friction force and the distance traveled. In the case of our beam-column, the friction force is $f(x)$ and the distance is the relative displacement between the two beams u, therefore the work done

$$U_f = -\int_{t_1}^{t_2}\int_0^l \mu q(x) u dx dt, \tag{7}$$

where μ is the coefficient of friction. Now, we need to determine U_f in terms of the beam-column vibration using Eq. 1. Under pure bending and the full slip regime we asume $u_1 = u_2 = 0$ (Fig. 3), u can be rewritten in terms of w

therefore Eq. 7 becomes

$$U_f = -\int_{t_1}^{t_2}\int_0^l \mu q(x) T w' dx dt$$
$$= \int_{t_1}^{t_2} \mu q(x) T W(t) dt. \quad (8)$$

At this stage, we have the energy quantities and we need to apply it to our beam-column. To analyse the effect of the energy dissipation on the beam-column vibration, we write the energy expressions at time t_i at full deflection as shown in Fig. 5 where the beam-column has no kinetic energy and $t_{i+1} = t_i + \pi/w_n$ (after half a period, where again the beam-column has no Kinetic energy). Then we apply the energy conservation principle which results in

$$(\frac{EI\pi^2}{32l})(W_{i+1}^2 - W_i^2) = \mu q(x)\frac{T}{w_n}(W_{i+1} - W_i), \quad (9)$$

where W_i is the tip deflection at time t_i and W_{i+1} at t_{i+1}. If the deflection W_i is known, equation 9 can be used to predict the deflection W_{i+1} at time t_{i+1}. Therefore Eq. 9 can be used to predict the maximum deflection of the beam-column in every half period increment.

2.4. Simulation Of The Energy Balance Model

The theoretical model was simulated in a Matlab program . Initially the envelope of vibration is determined which is based on the dominant damping. During the cycles where friction damping is predominant, Eq. 9 was modified to calculate the magnitude of successive half periods as follows:

$$W_{i+1} = \begin{cases} \frac{32l\mu T}{EI\pi^2 w_n} q(x) - W_i, & if\ W_i \geq 0 \\ \\ -\frac{32l\mu T}{EI\pi^2 w_n} q(x) - W_i, & if\ W_i \leq 0. \end{cases} \tag{10}$$

Eq. 10 are used to determine the maximum deflection over every half a period of time as shown in Fig. 5. During cycles where the beam-column is in stick phase, the envelope was based on only viscous damping which was determined experimentally (Fig. 13). To define the transition between predominant friction damping to viscous damping, we need to know the conditions that cause the transition from slip to stick. From Eq. 10 we can see that the friction damping is no longer effective when

$$|W_i^*| \leq \frac{8l\mu T}{EI\pi^2 w_n} q(x), \tag{11}$$

2.5. Dynamic Response Model

In this section, we determine the structural properties of the beam-column. First, we relate the internal forces and reactions within the structure to its deflection under different friction regimes. The forces acting along the beam-column are shown in the free body diagram of a differential element in Fig. 6. The beam-column is assumed to be under a transverse and an axial loading.

Fig. 6 shows that the forces P and V and moment M acting on the whole structure can be expressed in terms of internal forces acting on each beam

separately. The internal moments acting on each beam are still taken about the neutral axis of the whole structure. The moment acting on the whole structure on the left hand side can be expressed in terms of the internal forces and moments as follows

$$M = M_1 + M_2 + P(T - h) - P_1 T, \tag{12}$$

where T is the distance between the centrelines of the two beams and h is the distance between the centreline of the top beam and the neutral axis of the structure (Fig. 6). Note also $P = P_1 + P_2$.

The reactions within each beam can be related to its deflection by considering compatibility, i.e the lateral deflection at any point on the top beam is equal to the deflection of the lower beam. This can be expressed using beam theory [15] as follows

$$\frac{d^2 w}{dx^2} = w'' = -\frac{M_1}{E_1 I_1} = -\frac{M_2}{E_2 I_2}. \tag{13}$$

Combining Eq. 12 and 13 results in

$$w'' = -\frac{M - P(T - h) + P_1 T}{E_1 I_1 + E_2 I_2}. \tag{14}$$

In Eq. 14, P_1 is unknown and further assumptions are needed to define it. Differentiating P_1 and P_2 with respect to x will result in the friction force at the interface per length, $f(x)$ [1]

$$P_1' = -f(x), \tag{15}$$

and

$$P_2' = f(x). \tag{16}$$

From this point on, the beams are assumed to be identical, i.e. $A_1 = A_2 = A$ and $I_1 = I_2 = I$.

Differentiating Eq. 14 with respect to x and combining it with Eq. 15 results in

$$f(x) = \frac{2EA}{T} W''' + \frac{1}{T} M'. \tag{17}$$

It should be noted that P is constant along x. Differentiating Eqs. 2 and 4, and combining them with Eqs. 3, 15 and 16 leads to

$$f(x)'' = k\frac{2}{EA} f(x) + kTw'''. \tag{18}$$

Combining Eqs. 17 and 18 results in

$$w'''' - k\alpha w'' = k\beta M - \lambda M'', \tag{19}$$

where for identical beams $\alpha = \frac{1}{2E}(\frac{AT^2+4I}{AI})$, $\beta = \frac{1}{E^2IA}$ and $\lambda = \frac{1}{2EI}$.

All the equations, derived so far, describe static conditions. To describe dynamic conditions we relate the moment to the dynamic deflection. Under free vibration, the moment is related to the transverse displacement as follows [15]

$$\frac{\partial^2 M}{\partial x^2} = -m\frac{\partial^2 w}{\partial t^2}, \tag{20}$$

where m is the mass per unit length of the beam.

2.5.1. The effect of friction on the beam-column dynamics

Defining the constant of friction k is one task that can be done only experimentally therefore it will be assumed to take different values depending on the friction-displacement relation described in Fig.4. The friction-displacement parallelogram can be divided into sticking and slipping phases. During the sticking phase, the two beams act as one. Therefore, we assume that the change in relative displacement u is negligible regardless of the friction force magnitude $f(x)$. Consequently $k \to \infty$, and equation 19 can be rewritten in the following form

$$w'' = -\frac{\beta}{\alpha} M. \tag{21}$$

Differentiating Eq. 21 twice with respect to x and combining it with Eq. 20 results in

$$\frac{\partial^4 w}{\partial x^4} = -\frac{2m}{E(4I + T^2 A)} \frac{\partial^2 w}{\partial t^2}, \quad \text{if } f(x) \geq \mu q(x) \ . \tag{22}$$

Eq. 22 describes the transverse vibration of a single beam with the same size of our beam-column with no viscous damping. This means that in the absence of slip at the interface, the beam-column acts as a single beam. Equation 22 can be solved exactly — see for example [16].

The second phase in the friction-displacement parallelogram is the slipping phase which is only achievable if the static friction between the columns is overcome, i.e.

$$f(x) \geq \mu q(x), \tag{23}$$

where $q(x)$ is the loading applied by the bolts. To operate effectively, the bolted friction beam-columns must be designed with the appropriate bolt tensions to dissipate significant vibration energy when dynamically excited. The tension in the bolts needs to be selected to allow slipping to take place under external vibration. Therefore, it is required to define the relation between the beam dynamics and the bolt tension. First, the friction force $f(x)$ at the interface needs to be expressed in terms of the moment as follows

$$f(x) = \frac{TA}{T^2A + 4I} M'. \tag{24}$$

Combining Eq. 23 and 24 results in the optimal load $q^*(x)$ at which the beam-column transfers from slip to stick

$$q^*(x) \leq \frac{TA}{\mu(T^2A + 4I)} M'. \tag{25}$$

Once the bolt tension reaches the optimum value the beam-column crosses from slipping to sticking phase. During the slipping phase the friction force is assumed to be constant regardless of the magnitude of the relative displacement, therefore $k \to 0$. The differential equation Eq. 19 can be simplified to the following form

$$w'''' = -\lambda M''. \tag{26}$$

At this stage the neutral axis moves from the single line in Fig. 6 to two different neutral axes within each beam. We assume that the beams still have the same vibration mode. Combining eq. 20 and 26 results in

$$frac\partial^4 w\partial x^4 = -\frac{m}{2EI}\frac{\partial^2 w}{\partial t^2}, \quad \text{if } f(x) \geq \mu q(x) \ . \tag{27}$$

Eq. 27 represents the vibration of a beam with a bending stiffness double the stiffness of each column and it can be solved exactly see for example [16].

2.6. Simulation Of The Dynamic Response Model

As noted earlier, the model described in Sec. 2.4 provides amplitude data at a time resolution of half a period. In order to calculate the response at a higher time resolution a time stepping simulation was developed. The rest of the modeling in Fig. 5 was based on a time step calculation. Every step of time Δt the friction force at the interface is calculated. Then the stick-slip phase is determined based on equation 1 and the stiffness of the column is calculated as well as the frequency of vibration as explained in Sec. 2.5. Then, the temporal function of the vibration,, is calculated using the following Eq.

$$w = W * (\cos(w_n t - \Phi)), \tag{28}$$

where W is the maximum deflection in every period of time calculated from Eq. 10, w_n is the natural frequency and Φ is the phase shift calculated based on the change in stiffness that occurs from one time step to another.

Once the tip of the beam deflection is defined, the relative displacement

during full slip phase is then calculated based on Eq. 1. During full stick, it is calculated based on

$$u_i = u_{i-1}, \tag{29}$$

where u_i, u_{i-1} are the relative displacement at time t_i and time t_{i-1}.

The theoretical models in Fig 9 and 10 are calculated using this model.

3. Experimental Results

3.1. Set Up

The experimental set up consists of a single friction column composed of two beams (Fig. 7) pressed against each other using a set of three bolts. The properties of each beam are listed in appendix A. We monitored the normal pressure applied by the bolts using load cells. The beam column pressure was increased gradually and from $0N$ to $140N$ per bolt. Every time the tension in the bolts was increased, we deflected the column and released it from the deflected position. The velocity at which the structure vibrates was measured using a laser vibrometer as shown in Fig. 7. We also installed a number of strain gauges on the outer surfaces of the beams as shown in Fig. 7 to monitor the stress magnitudes as the beam-column vibrates.

The relative displacement between the two beams was measured using a linear variable differential transformer (LVDT) that was attached at the top

of the beam-column as shown in Fig. 7. The top part of the LVDT was fixed to the outer surface of beam 1 while the bottom part of it was fixed on the outer surface of $beam_2$, see Fig. 8 The measurements taken from the LVDT give the total slip from the clamped end up to the point where the LVDT is installed during the full slip phase. During full stick phase, the LVDT is supposed to record zero as the lateral planes remain normal to the neutral axis of the beam.

4. Results and Discussion

4.1. Relative Displacement Results

The relative displacement depends on the friction dynamics in the column as described in Sec. 2.1. The experimental results show three cases. First, under low bolt tension, the structure is in full slip condition all the time (Fig. 9(a)). At this stage, the relative displacement measured by the LVDT shows a good agreement with the theoretical values calculated from Eq. 1. Under high bolt tension the column is in stick mode all the time (Fig. 9(c)). The relative displacement measured by the LVDT at this stage is due to the slip that takes place between the top bolt and the position of the LVDT. In between the two extreme cases, the column crosses from stick to slip mode in every period of vibration. The relative displacement measurements taken by the LVDT, displayed in Fig. 10, show that for low bending velocity the

column is in sticking regime and when the velocity reaches the maximum value the column switches to slipping regime.

The theoretical model is a combination of the slip then stick motion based on Eq. 24 and when this reaches the requirement in Eq. 23, the column starts to slip.

The difference between the measurement and theoretical relative displacement in Fig. 10(a) and (b) is due to the fact that during slipping condition, the column is not really in full slip whereas the theoretical simulations assume full slip.

4.2. Validation Of The Theoretical model

The mechanical properties of the specimen used in both the experimental set up and modeling are given in Fig. 7.

Eq. 10 was used in a numerical model repeatedly to determine the envelop of vibration as explained in Sec. 2.4. Despite the simplicity of the model, it is clear that the theoretical predictions agree very well with the experimental results. For example, we can see in Fig. 11 that the vibration magnitude and duration is visibly reduced as the load $q(x)$ is increased. After a number of cycles it seems that the experimental results converge to zero whereas the theoretical predictions continues to have a small oscillation. The reason for that is that during the first cycles of vibration, the friction damping is dominant therefore it shows good agreement with the theoretical

predictions. However, when a certain magnitude of vibration is reached, slip (i.e dynamic friction) no longer occurs and the friction damping drops quickly to near zero. At this stage the beam-column starts acting as a single beam with predominant viscous damping which is not included in theoretical modeling. where W_i^* is the critical vibration amplitude at which the slip to stick transition occurs. It can be seen that increasing the bolt tension $q(x)$ results automatically in the increase of W_i^*. As the bolt tension increases, more relative displacement is required for slip to occur. Hence, slip starts failing at higher vibration magnitudes, and the column starts behaving as a single beam with only viscous damping. This can be clearly seen in Fig. 11(b), where slip fails at higher vibration amplitudes and friction damping becomes increasingly less effective. Consequently, vibration takes increasingly longer to converge when bolt tension is increased.

4.3. Frequency analysis

The frequency at which the column vibrates is a proportional to its stiffness. From Eq. 22 and 27, the column stiffness during full stick condition is double its value during full slip. Therefore, the natural frequency of the beam-column vibration is expected to double as it operates within the sticking phase. This analysis was confirmed by the frequency analysis run on the experimental results and shown in Fig. 12(a). Before the full stick status is reached, the dominant frequency increases gradually as shown in Fig. 12(b).

Taking the frequency of the whole time response in one does not show how the frequency changes for a given bolt tension, it merely reveals the dominant frequency (Fig. 12). Inspection of results from column vibrating within stick-slip condition shows that over a single cycle of vibration, the frequency starts closer to the full slip case, i.e. low frequency. As the maximum deflection per cycle decreases the column goes into the full stick regime therefore the frequency increases (Fig. 14(b)).

4.4. Damping properties

The presence of dynamic friction at the interface has clearly improved the damping in the structure. Friction damping is typically characterized by a linear decay envelope of the vibration until a threshold for sticking is achieved and dynamic friction fails [17]. However in order to compare with viscous damping, we approximate the decay by an exponential decay curve over the first three periods of vibration as shown in Fig. 13(a). The equivalent damping ratio as the bolt tension is increased is displayed in Fig. 13(b). The equivalent overall damping displayed in Fig. 13(b), shows a significant improvement of the damping properties in the beam-column when the bolt tension is properly adjusted. in fact, the equivalent damping ratio around the optimum bolt tension is approximately ten times higher than the inherent damping of the beam-column.

5. Conclusions

This paper includes an analysis of the friction damping present in a column composed of two beams bolted together. The analysis and the experimental results confirmed that dynamic friction can be used to improve the damping properties of the beam-column considerably. A full analysis was provided explaining the effect of friction on the dynamics of the beam column and how that changes as the tension in the bolts is varied. Under low bolt tension, the column has the properties of a single beam with normal exponential decay whilst for high bolt tension, the column has the properties of a beam twice as thick as a single beam. This was confirmed by the changes in natural frequency of the beam-column under both conditions. During the cycles where dynamic friction is present and bolt tension is appropriately adjusted, friction damping can be as much as ten times higher than the inherent viscous damping.

ACKNOWLEDGMENTS

Hadjila Bournine is sponsored by the Algerian ministry of higher education and scientific research.

References

[1] L.Panning, K.Popp, W.Sextro, Vibration damping by friction forces: Theory and applications. *Journal of Vibration and Control*, 9:419–448, 2003.

[2] S.P.Timoshenko, *History of strength of materials :with a brief account of the history of theory of elasticity and theory of structures*. McGraw-Hill, 1953.

[3] I.H.Mualla, B.Belev, Performance of steel frames with a new friction damper device under earthquake excitation. *Engineering Structures*, 24(3):365–371, March 2002.

[4] J.H.Park, B.W.Moon , K.W. Min, S.K. Lee, C.K Kim, Cyclic loading test of friction-type reinforcing members upgrading wind-resistant performance of transmission towers. *Engineering Structures*, 29(11):3185–3196, November 2007.

[5] C.G.Cho, M.Kwon. Development and modeling of a frictional wall damper and its applications in reinforced concrete frame structures. *Earthquake Engineering & Structural Dynamics*, 33(7):821–838, 2004.

[6] C.E.Grigorian, E.P.Popov, T.S. Yang, Developments in seismic struc-

tural analysis and design. *Engineering Structures*, 17(3):187–197, April 1995.

[7] Z.M.Law, S.S.Wu, S.L.Chan, Analytical model of a slotted bolted connection element and its behaviour under dynamic load. *Journal of Sound and Vibration*, 292(3-5):777–787, May 2006.

[8] Y.C.Kurama, B.G.Morgen, Characterization of two friction interfaces for use in seismic damper applications. *Materials and Structures*, 42:3549, 2009.

[9] L.Gaul, R.Nitsche, Friction control for vibration suppression. *Mechanical Systems and Signal Processing*, 14(2):139–150, March 2000.

[10] R.Nitsche, L.Gaul, Smart friction driven systems. *Institute of physics publishings, smart materials and structures*, 14:231236, 2005.

[11] S.Hurlebaus, J.Wirnitzer , L.Gaul, H.Albrecht, Enhanced damping of lightweight structures by semi-active joints. *Acta Mechanica*, 195(1-4):249–261, 2008.

[12] B.F.Jr.Spencer, S. Nagarajaiah, State of the art of structural control. *Journal of Structural Engineering*, 129(7):845–856, 2003.

[13] D.J. Segalman, Modelling joint friction in structural dynamics. *Structural Control and Health Monitoring*, 13(1):430–453, 2006.

[14] E.J.Berger, Friction modeling for dynamic system simulation. *Applied Mechanics Reviews*, 55(6):535–577, 2002.

[15] J.M.Gere, *Mechanics of materials*. Thomson, Book/cole, 6th edition, 2004.

[16] W.T.Thomson, M.D.Dahleh, *Theory of vibration with applications*. Chapman & Hall, 1993.

[17] L.N.Virgin, *Introduction to Experimental Nonlinear Dynamics*. Cambridge University Press, 2000.

List of Figures

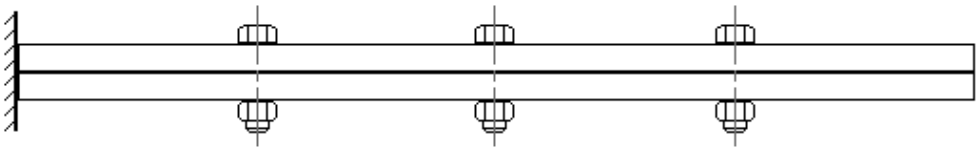

Figure 1: Bolted friction beam-column, with two beams and three bolts.

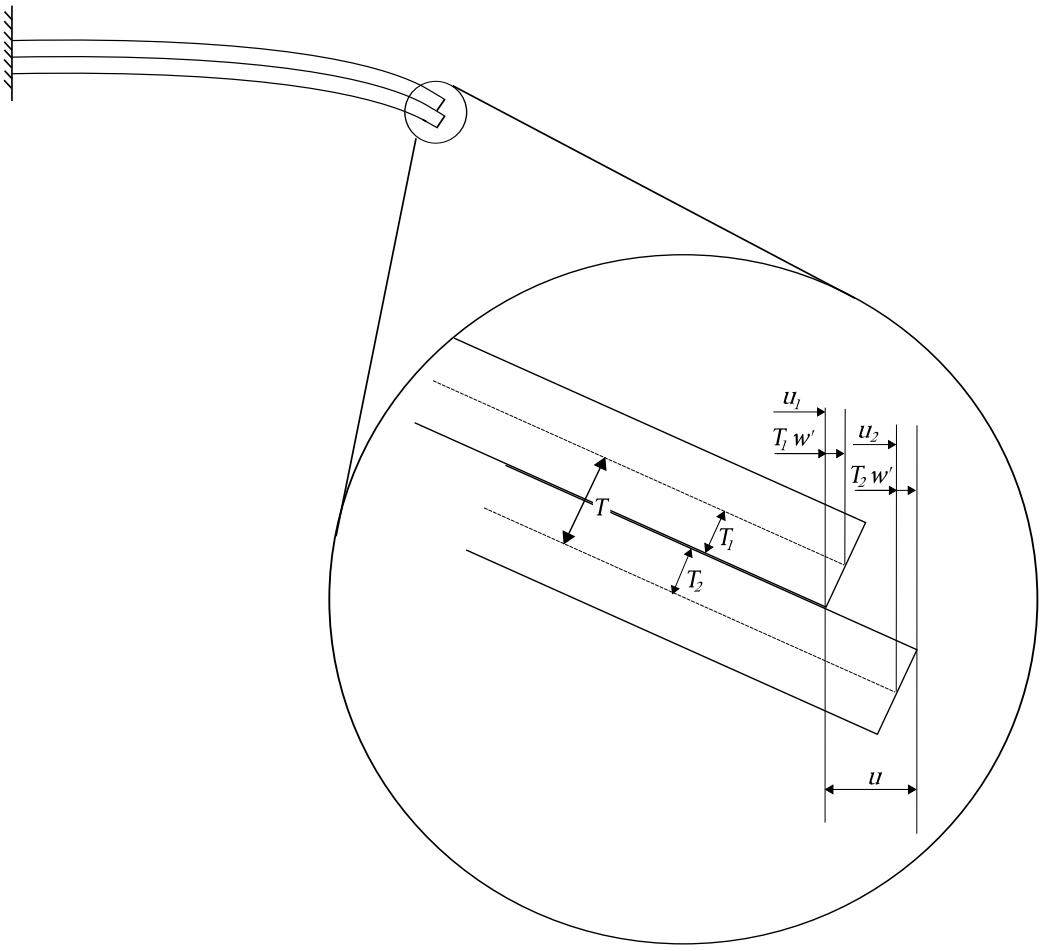

Figure 2: The total relative displacement between the two beams at the free end of the column.

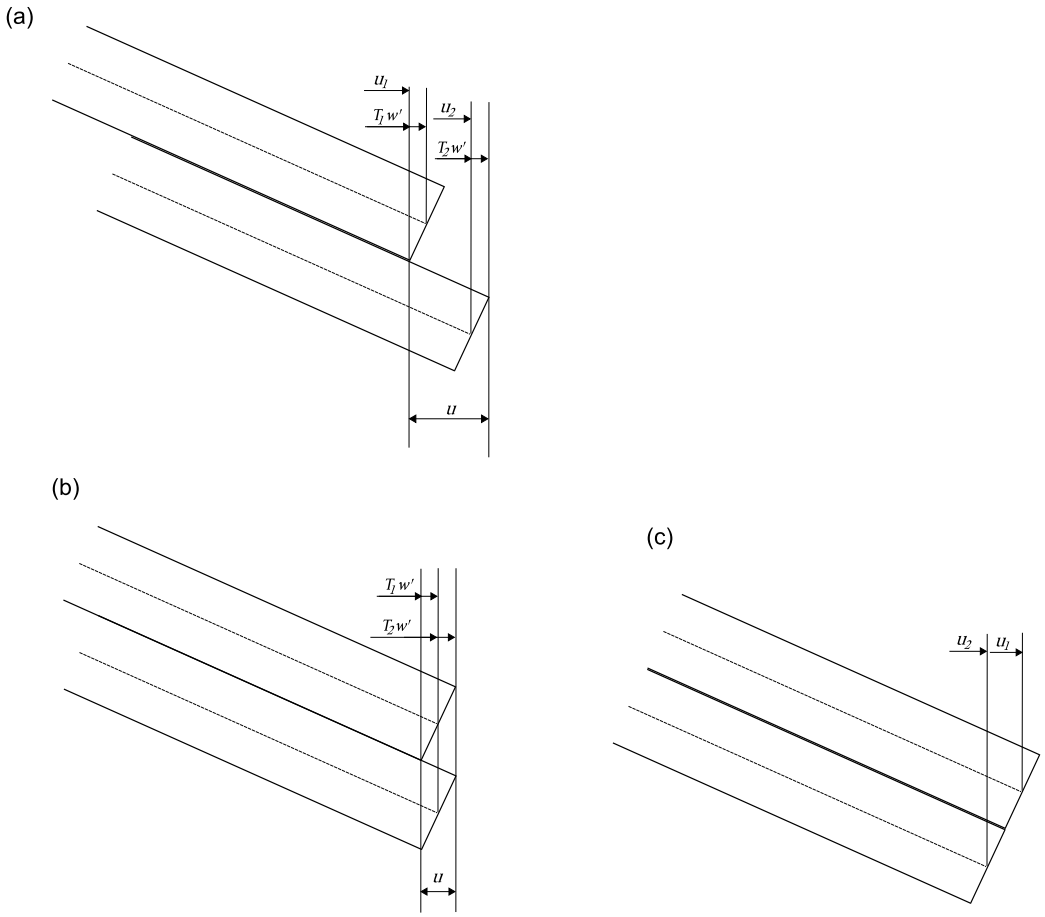

Figure 3: The total relative displacement between the two beams at the free end of the column, (a) The general case, the beam under axial loading and bending, (b) under pure bending and full slip, (c) under pure bending and full stick.

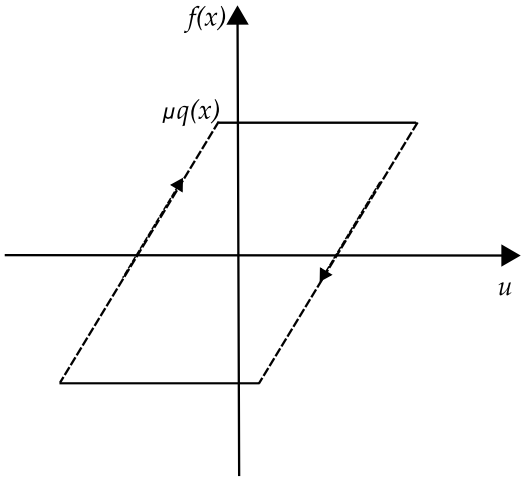

Figure 4: The assumed friction model, − − − sticking phase, — slipping phase.

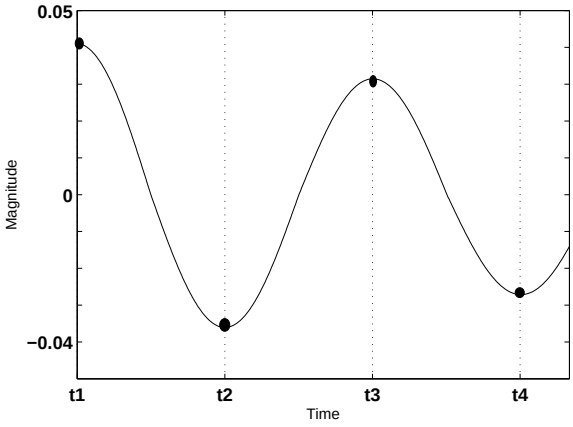

Figure 5: The model simulation, • defined using the energy balance model, — calculated using dynamic response model.

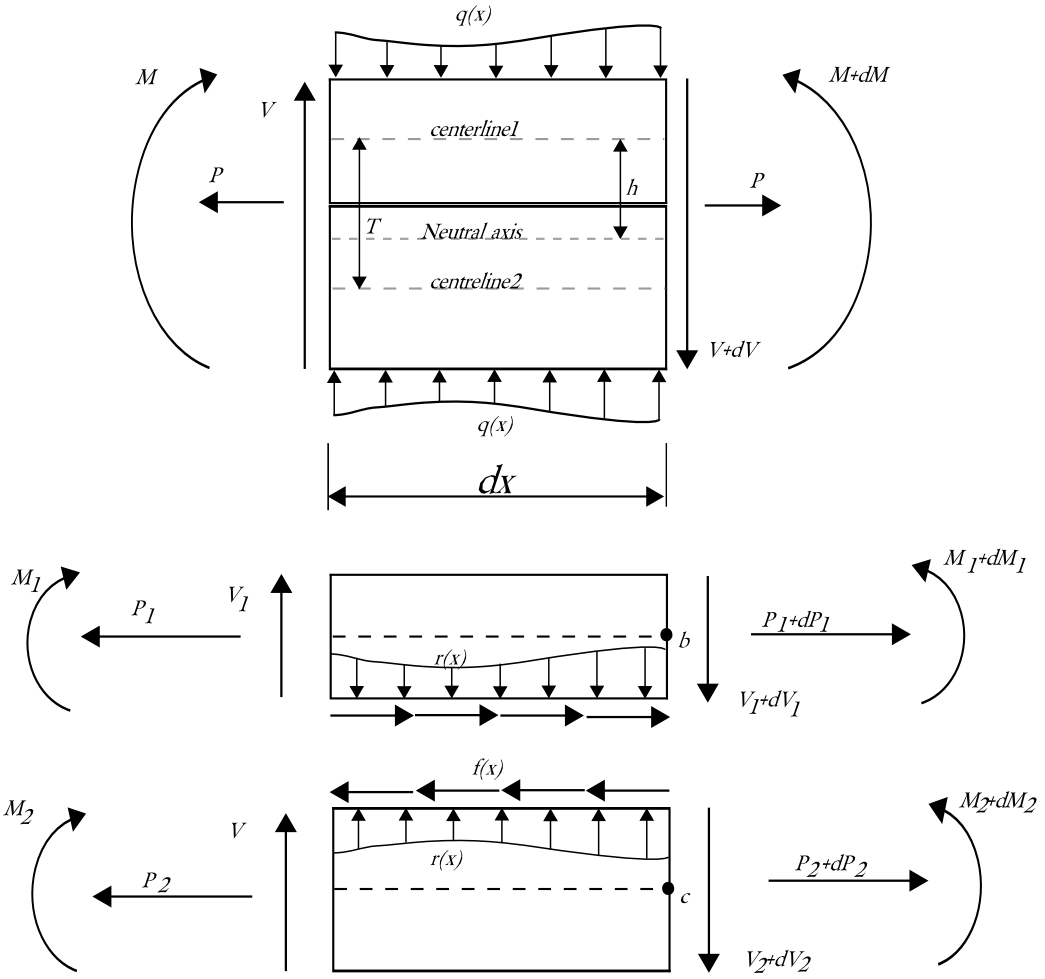

Figure 6: The forces acting withing the beam-column

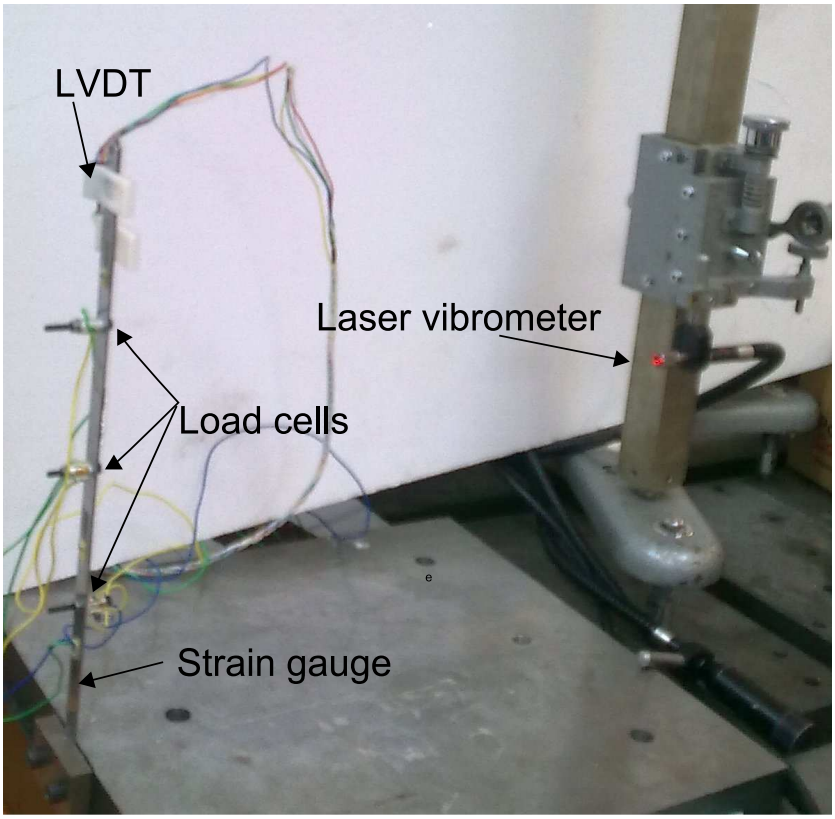

Figure 7: The experimental set up, column dimensions: $0.3m \times 0.0125m \times 0.0005m$, Young's modulus : $E = 167GPa$, Density: $\rho = 6970kg/m^3$ and coefficient of friction: $\mu = 0.3$.

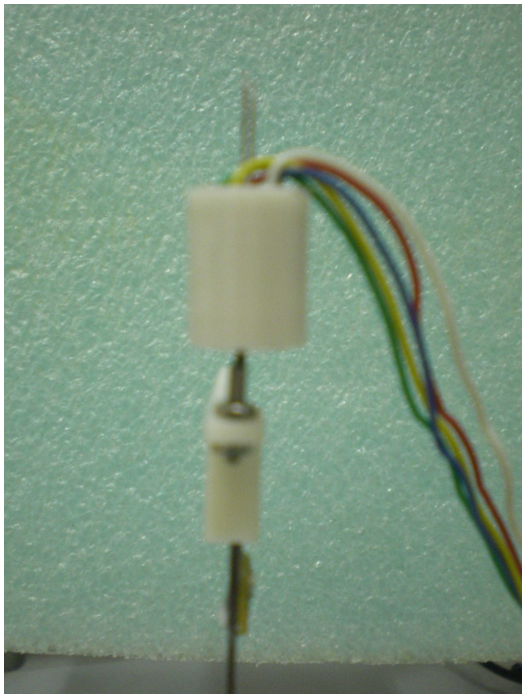

Figure 8: The LVDT used in the experiments.

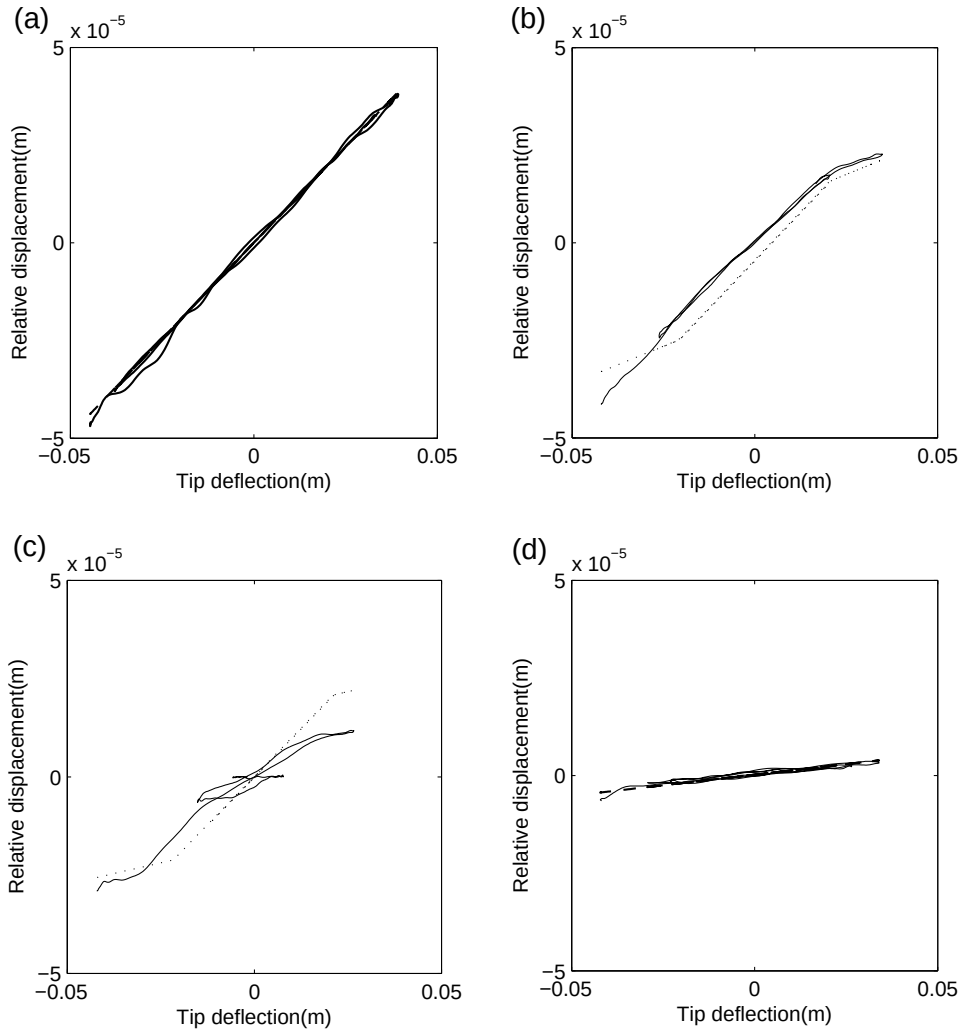

Figure 9: The total relative displacement between the two beam-columns at the free end of the column versus the tip deflection, (a) average bolt tension 0 N, (b) average bolt tension 23 N, (c) average bolt tension 36N, (d) average bolt tension 112N.
− − − theoretical value based on the theoretical tip deflection, ——— the relative displacement measurement from the LVDT .

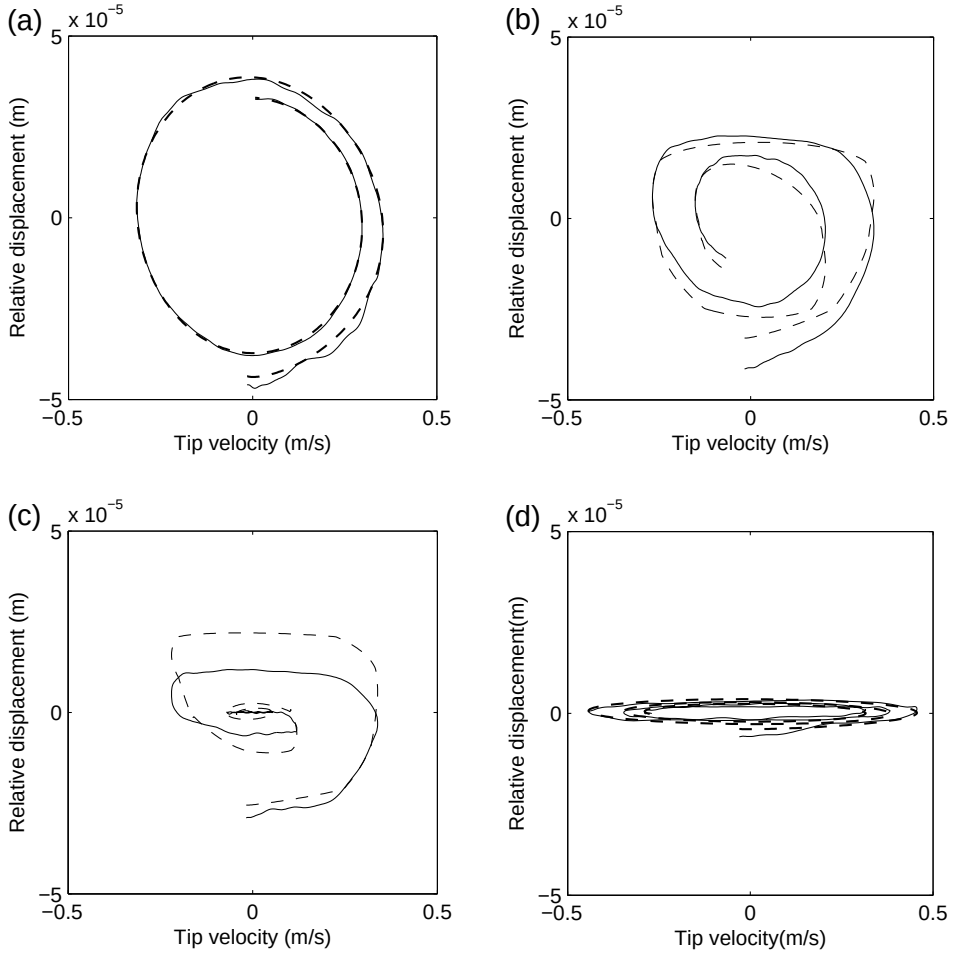

Figure 10: The total relative displacement between the two beam-columns at the free end of the column versus tip velocity, (a) Average bolt tension 0 N, (b) average bolt tension 23 N, (c) average bolt tension 36N, (d) average bolt tension 112N.

– – – theoretical value based on the the theoretical tip deflection, —— the relative measurement as measured by the LVDT.

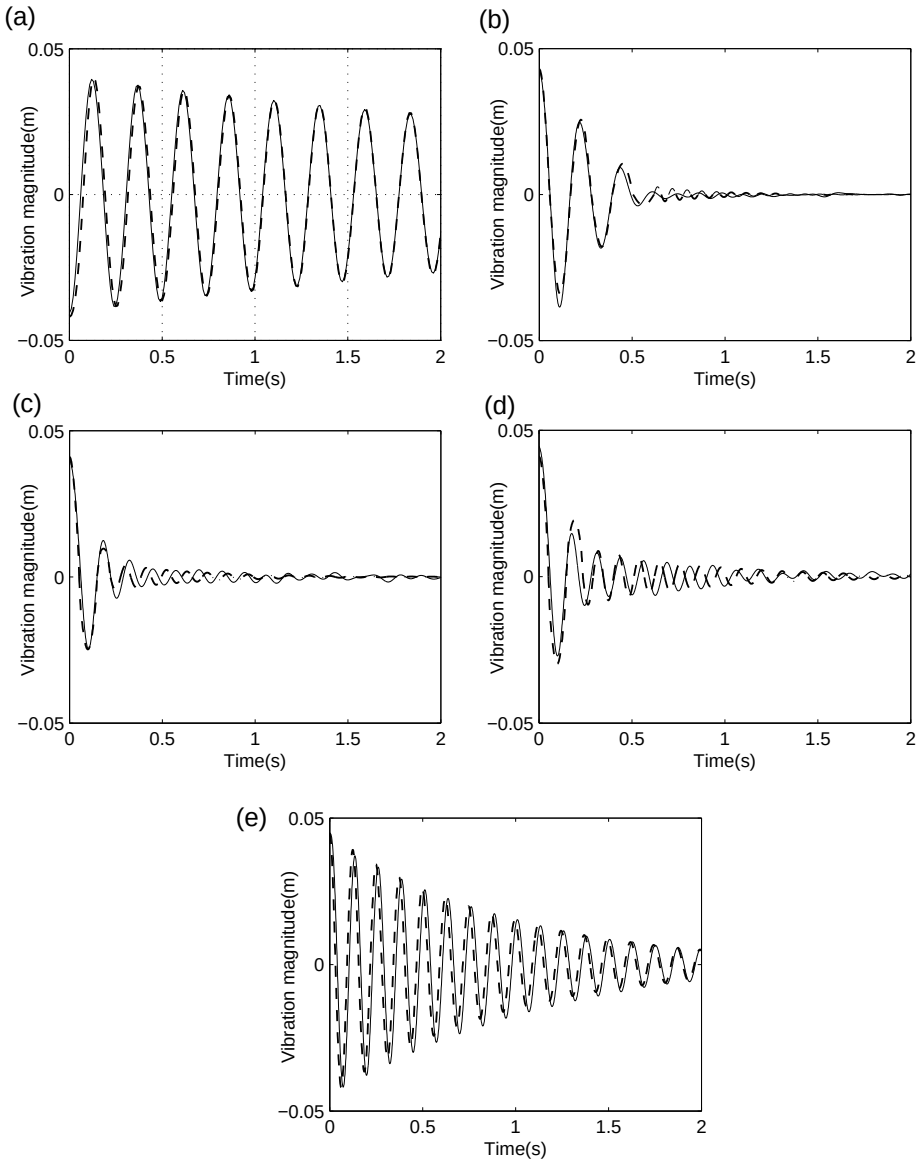

Figure 11: The dynamics of the beam-column as the tension in the bolts is increased, (a) average bolt tension= 0 N, (b) average bolt tension= 17.3 N (c) average bolt tension = 33.1 N(d) Average bolt tension = 46 N (e) average bolt tension = 112N

− − − theoretical values , ——— the relative displacement measurement from the LVDT.

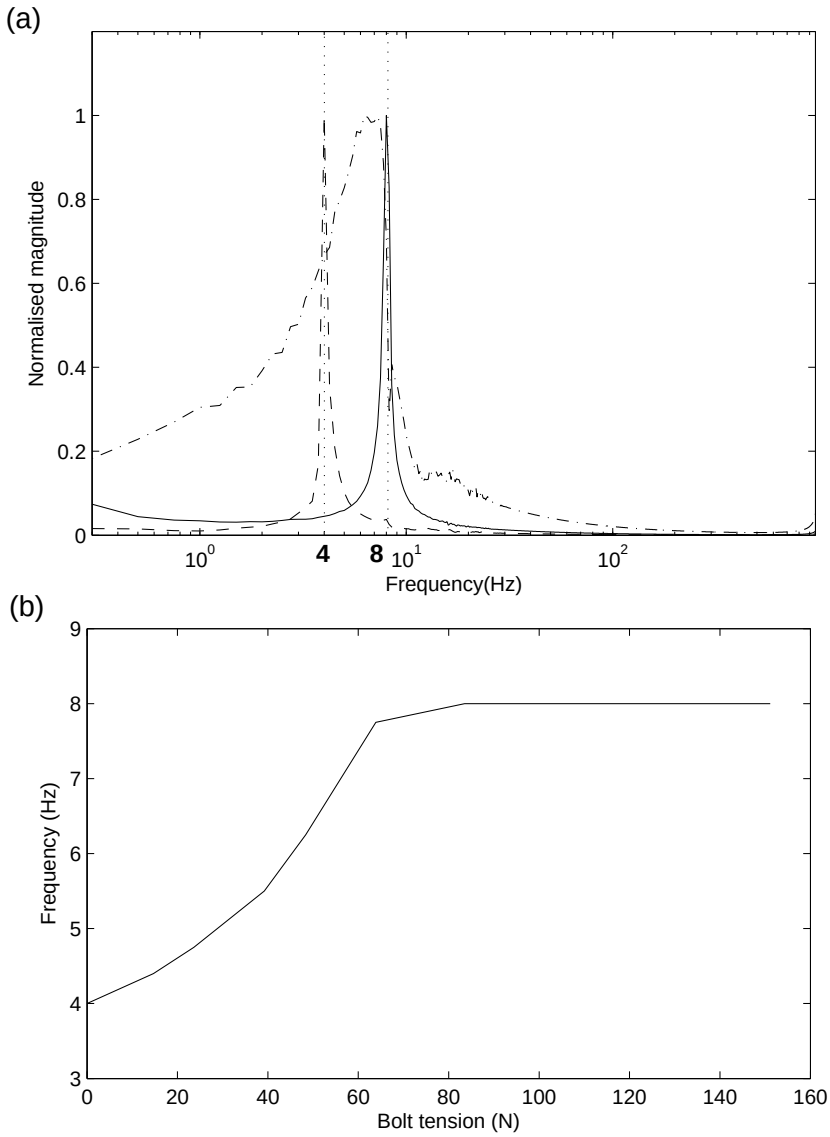

Figure 12: The vibration frequency of the beam-column under different bolt tensions, (a) shows the natural frequency for: $- - -$ bolt tension 0N, $- \cdot - \cdot -$ bolt tension 33.1 N, —— bolt tension 112N. (b) the dominant frequency as bolt tension is varied.

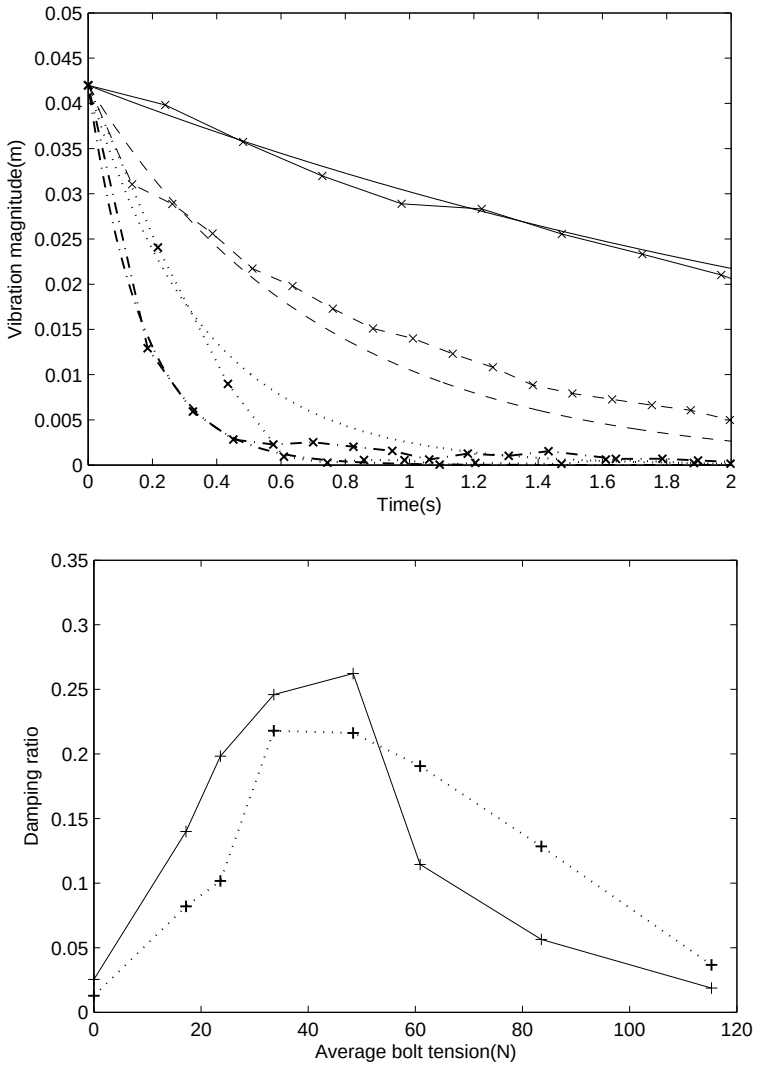

Figure 13: The effect of bolt tension on the damping ratio and vibration frequency, (a) the signal envelope, —×— bolt tension= $0N$,— $\zeta = 0.0128$, $--\times--$ bolt tension= $112N$, $---$ $\zeta = 0.0349$, $\cdot\cdot\times\cdot\cdot$ bolt tension= $17.3N$, $\cdots$ $\zeta = 0.0917$, $-\cdot\times\cdot-$ bolt tension= $33.1N$, - $\cdot-$ $\zeta = 0.2216$. (b) damping ratio vs bolt tension, — equivalent damping ratio over the whole vibration time, $\cdots$ equivalent damping ratio over the first three periods of vibration.

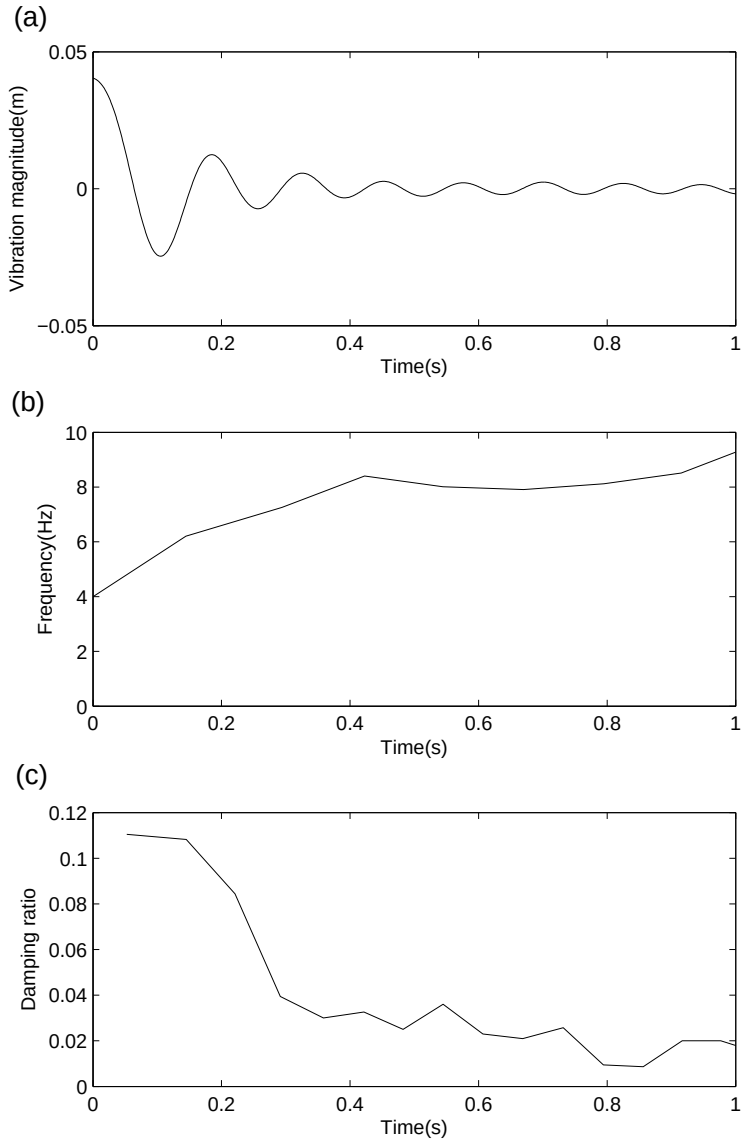

Figure 14: The frequency and damping changes over time under an average bolt tension of 33.1 N (a) vibration amplitude over time (b) frequency change over time, (c) damping ratio over time.